A mechanical model for fibres of linear polyethylenes over a wide range of crystallinities

J. M. Rossignol*, R. Seguela† and F. Rietsch
Laboratoire de Structure et Propriétés de l'Etat Solide, URA CNRS 234, Université de Lille I, 59655 Villeneuve d'Ascq Cedex, France
(Received 25 July 1989; revised 12 September 1989; accepted 11 October 1989)

The Takayanagi-like mechanical model introduced by Grubb for semicrystalline high-modulus fibres is used for linear polyethylenes covering the range of crystal weight fraction 0.28–0.66. This model assumes an interruption of crystal continuity in the mechanically active part of the fibre, which is consistent with the relatively high elasticity of the fibres from medium- and low-crystallinity materials. A novel method is proposed for determining the fraction f of the interrupting amorphous phase from the stress–elongation curves of the fibres assuming a Gaussian behaviour at low strains. A universal relationship is found between f and the compliance of the fibres. The volume fraction of the mechanically active part of the fibres is shown to decrease along with the decreasing crystallinity of the starting materials, indicating a gradual reduced capability to undergo a fibrillar transformation.

(Keywords: ethylene copolymers; fibres; mechanical model; tensile modulus; stress–strain behaviour)

INTRODUCTION

Modelling is a natural stage in the search to understand the structure–mechanical property relationships of solid polymers. Fibres from semicrystalline polymers have received much attention in this regard, notably high-density polyethylene, which led to high-modulus and high-strength fibres. Peterlin has laid down the pioneer 'fibrillar model' based only on structural grounds[1,2], in the case of solid-state drawing, by the combination of extensive X-ray diffraction studies, electron microscopy, infra-red spectroscopy and thermal analyses. A number of different structural models have been developed for fibres processed by melt extrusion[3–7] or solution spinning[8,9], but all models contain fibril-like structural units with various arrangements of lamellar counterparts.

In parallel, mechanical models for fibres have been derived from the structural analogues[2,10–13]. These mechanical models involve some of the main structural features of the fibres such as chain orientation, crystallite dimensions, crystal–amorphous long period and crystallinity, together with the intrinsic elastic moduli of the various phases. Generally, a continuous structure of perfectly oriented chains has been assumed to account for the ultra-high modulus of highly drawn fibres, which is currently in the range 50–150 GPa[12–22] depending on the process, starting material, drawing temperature, molecular weight, etc. This assumption involves either taut tie molecules between lamellar crystals as proposed by Peterlin[2], or needle-like crystals as suggested by Barham and Arridge[11] or crystalline bridges according to Gibson *et al.*[12]. Grubb[13] proposed an alternative model, which assumes that the fibrillar crystals contain defective regions made of entanglement clusters that interrupt the crystal continuity. The Takayanagi-like scheme of this model shown in *Figure 1* consists of a 'series' and 'parallel' coupling of the various parts of the fibre. The left-hand branch of the model relates to the fibrillar crystals of volume fraction b with respect to the whole material in which the defective regions of entanglement clusters have a volume fraction f and an intrinsic modulus E_1. The right-hand branch corresponds to the stacking of lamellar crystals and amorphous layers along the fibre axis. The overall crystallinity is X_c, and E_c and E_a are the intrinsic moduli of the crystalline and amorphous phases.

Some comments must be made about this model. The first point is that the complete separation of fibrillar and lamellar components relies on the well known shish-kebab structure of melt- and solution-spun fibres involving chain-extended crystals and overgrown lamellar crystals[13]. But the analogy is not obvious in the case of solid-state drawing, which proceeds through a fragmentation of the large crystalline lamellae and a concomitant pulling out of the intercrystalline tie molecules and entangled chain folds from the fracture surfaces, partially unfolding the chains parallel to the draw direction[2]. However, the remaining chain-folded crystal blocks, which cannot transmit the stress directly through their fold surfaces, may be associated with the lamellar component of the model. The unfolded chains partially recrystallized during the drawing process constitute the fibrillar component. The second point to be mentioned is that only the crystal continuity is interrupted in Grubb's model. The fibrillar continuity necessary to transmit the load throughout the fibre is still preserved by means of crystalline bridges or taut tie molecules lying between the adjacent fibrils.

In a study concerned with the drawing behaviour of a linear low-density polyethylene (LLDPE)[23], we reported that the fibres exhibit original mechanical properties, i.e. a good tensile strength $\sigma_R \approx 0.6$ GPa associated with a rather high modulus $E \approx 10$ GPa and a large residual

* Present address: ATOCHEM Research Centre, Serquigny, France
† To whom correspondence should be addressed

0032-3861/90/081449-07

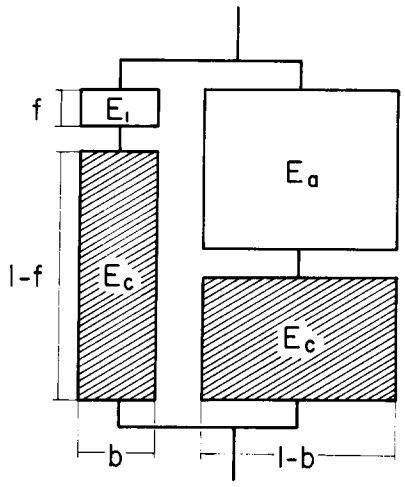

Figure 1 Modified Takayanagi-like model for semicrystalline high-modulus fibres according to Grubb[13]

elasticity $\varepsilon \geqslant 10\%$. This latter feature is particularly inconsistent with the mechanical models involving either crystal continuity or taut tie chains. But, on the other hand, Grubb's model can account for a large elasticity owing to the interruption of the crystal continuity by the defective amorphous regions in the fibrillar crystals. We have applied this model in the case of fibres drawn from LLDPE having a density $\rho = 0.930$[24,25]. Thanks to a novel method for determining the parameter f, we have established correlations between this parameter and the mechanical properties of the fibres. The success of this approach led us to extend our study to linear polyethylenes covering a wide range of crystallinities.

THEORETICAL CONSIDERATIONS

Tensile modulus

Takayanagi-like models are generally purely mechanical analogues for multiphase systems whose only elements of structural nature are the volume fractions of the different parts. The modified model proposed by Grubb (*Figure 1*) has additional structural bases, notably as concerns the 'parallel' coupling of two branches associated with the fibrillar and lamellar parts of the material. The modulus E for such an arrangement is:

$$E = b[(1-f)/E_c + f/E_1]^{-1} + (1-b) \times \{[X_c - (1-f)b]/(1-b)E_c + (1 - X_c - fb)/(1-b)E_a\}^{-1} \quad (1)$$

Considering that $E_a \ll E_c$ (see ref. 2 for instance), and assuming that $f \ll 1$, as will be shown later, the above equation can be reduced to:

$$E = b[(1-f)/E_c + f/E_1]^{-1} \quad (2)$$

This approximation is equivalent to neglecting the right-hand branch of the model, the left-hand branch being representative of the mechanically active part of the fibre. An additional simplification involving the previous assumption $f \ll 1$ can be introduced into equation (2), leading to the final relation for the modulus:

$$E = bE_c(1 + fE_c/E_1)^{-1} \quad (3)$$

Elongation ratio

The left-hand branch of the model of *Figure 1*, which corresponds to the mechanically active part of the fibre, is a 'series' phase coupling that obeys an additivity law of the elastic strains in the crystalline and amorphous phases, with coefficients respectively equal to the volume fractions of the two phases. This leads to the following strain-balanced equation:

$$\lambda_{macro} - 1 = (\lambda_c - 1)(1-f) + (\lambda_1 - 1)f \quad (4)$$

where λ_{macro} is the macroscopic elongation ratio applied to the fibre and λ_c and λ_1 are the respective elongation ratios of the crystalline and amorphous phases in the mechanically active part of the fibre. Taking into account that $\lambda_c - 1 \ll \lambda_1 - 1$, owing to the much greater stiffness of the crystal compared with the amorphous phase, equation (4) can be reduced to:

$$\lambda_{macro} - 1 = (\lambda_1 - 1)f \quad (5)$$

In fact, this latter relation only holds true if f is not too small; otherwise the two members of the right-hand side of equation (4) are of the same order of magnitude.

Stress–elongation curves

We have previously emphasized that the characteristic sigmoidal shape of the stress–elongation curves of the fibres from LLDPE is relevant to a rubber-like behaviour[24,25]. This is consistent with the fact that the left-hand side of the model of *Figure 1* represents the mechanically active part of the fibre, if one considers that the amorphous phase in polyethylene is rubbery at room temperature and that this latter is much more compliant than the crystal. It follows that, at low strain, the stress–elongation curves of the fibres should obey an equation derived from the Gaussian statistics of chains and having the general form[26]:

$$\sigma = A(\lambda_1 - \lambda_1^{-2}) \quad (6)$$

where σ is the stress per unit unstrained area in the amorphous fraction f of the mechanically active part of the fibre having an elongation ratio λ_1, and A is a constant characteristic of the molecular network at a given temperature. This treatment assumes that the fraction f is not constituted by entanglement clusters only, but also contains all unstrained chains in the form of slack tie molecules and entangled loose chain folds. From a strict mechanical standpoint, oriented amorphous chains such as taut tie molecules must be associated with the crystalline part of the fibrillar component of the model. Indeed, such molecules are not allowed to contribute to the elastic strain as long as the applied stress is lower than the level of the internal stresses that enforce the amorphous chain orientation within the fibre.

The tangent at the origin of the stress–strain relationship (6) has an equation:

$$\sigma = 3A(\lambda_1 - 1) \quad (7a)$$

or

$$\sigma = 3Af^{-1}(\lambda_{macro} - 1) \quad (7b)$$

Figure 2 shows that any arbitrary straight line of equation:

$$\sigma = B(\lambda - 1) \quad (8a)$$

or

$$\sigma = Bf^{-1}(\lambda_{macro} - 1) \quad \text{with } B < 3A \quad (8b)$$

has an intersection with the stress–elongation curve of

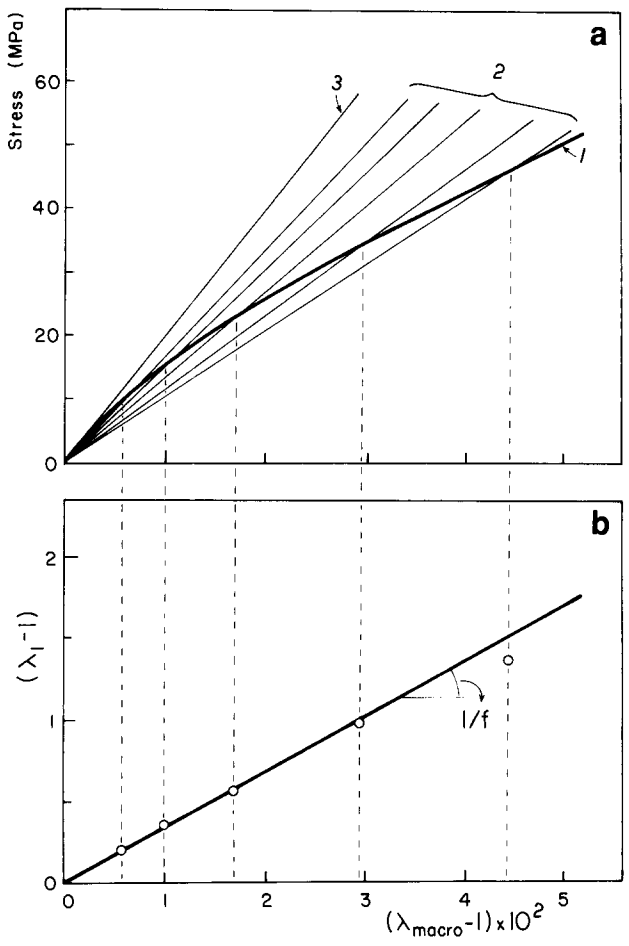

Figure 2 Determination method of fraction f in the case of a fibre from sample S4 having a draw ratio $\Lambda=7.3$. (a) Plots of (1) the experimental stress–elongation curve of the fibre, (2) a bundle of arbitrary straight lines following equation (8b) with various values of the constant B and (3) the tangent at the origin to the stress–elongation curve following equation (7). (b) Plot of the (λ_1-1) values computed from equation (9) as a function of $(\lambda_{macro}-1)$

the fibre, which must verify both equations (6) and (8a), and this leads to the following relation:

$$(\lambda_1-\lambda_1^{-2})/(\lambda_1-1)=B/A \qquad (9)$$

Numerical resolution of equation (9) gives a value of λ_1 for every B/A value, which can be determined graphically, according to *Figure 2a*, from the ratio of the slope of the arbitrary straight line (equation (8b)) to the slope of the tangent to the stress–elongation curve (equation (7b)).

The plot of (λ_1-1) as a function of $(\lambda_{macro}-1)$ gives a linear relationship as shown in *Figure 2b*, which supports *a posteriori* the assumption of 'Gaussian' behaviour for the active amorphous phase at low strains (viz. equation (6)). The value of fraction f can then be obtained from the slope of the graph of *Figure 2b* according to equation (5).

EXPERIMENTAL

Six 'linear polyethylenes' having roughly similar molecular weights and different densities (i.e. different crystal weight fractions) have been studied. These commercial-grade polymers are ethylene/1-butene random copolymers containing various concentrations of 1-butene units, which control the density. *Table 1* shows the molecular and physical characteristics of the samples.

The polymers were compression moulded at 160°C into sheets about 0.5 mm thick, and were allowed to relax at this temperature for 10 min before cooling at about 10°C min^{-1}. Dumbbell-shaped specimens with gauge dimensions 20×5 mm^2 were cut from the sheets and drawn at 80°C in an Instron tensile testing machine at a constant cross-head speed of 50 mm min^{-1}. The draw ratio is defined as $\Lambda=L/L_0$. The fibres having a gauge length of 50 mm were tested at room temperature using a cross-head speed of 1 mm min^{-1}. The tensile modulus was determined from the initial slope of the stress–strain curves of the fibres.

RESULTS AND DISCUSSION

The plots of the tensile modulus E *versus* draw ratio Λ for the six samples S1 to S6 are shown in *Figure 3*. The data have been reported on two separate graphs having different scales on the ordinate axis in order to provide better clarity in the range of low-modulus values. The plots exhibit a clear positive curvature, as already reported in our studies of the mechanical behaviour of fibres drawn from LLDPE[23–25]. A slight negative curvature of the E *versus* Λ plot has also been observed before reaching the maximum achievable draw ratio[24,25], namely for $\Lambda>11$. This is relevant to the formation of voids[27] as confirmed by the whitening of the fibres. Therefore, the present study has been limited to the range of draw ratios without whitening of the fibres.

In a recent paper, Leung *et al.*[28] reported Young's modulus data of oriented ethylene/1-butene copolymers determined from viscoelastic measurements at 10 Hz, in the range of draw ratios $1<\Lambda<9$. These data fall roughly into the range of our results, for samples having similar crystallinity. However, Leung *et al.* observed nearly linear relationships of E *versus* Λ, as has often been reported in the case of high-density polyethylenes[2,14–17,20,21], while

Table 1 Weight- and number-average molecular weights, $\bar{M}_w$ and $\bar{M}_n$, concentration of 1-butene comonomer, C_B, density ρ and crystal weight fraction X_c, of the polyethylene samples studied

Sample	Trade name	$\bar{M}_w\times10^{-3}$	$\bar{M}_n\times10^{-3}$	C_B (mol%)	ρ (g cm^{-3})	X_c[a]
S1	Eltex	157	30	0.6	0.950	0.66
S2	Marlex	178	19	1.1	0.943	0.62
S3	Lotrex	136	31	2.5	0.930	0.53
S4	Lotrex	140	29	5	0.919	0.43
S5	Norsoflex	161	32	8	0.910	0.34
S6	Norsoflex	148	35	12[b]	0.900	0.28

[a] Determined from differential scanning calorimetry according to ref. 23
[b] Sample S6 contains a few propylene units

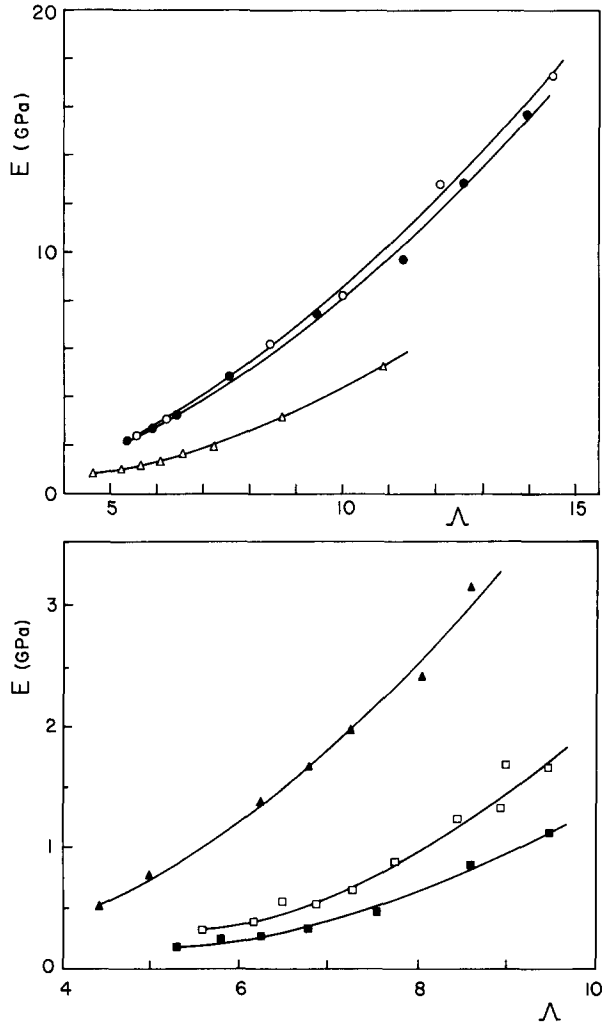

Figure 3 Plots of the tensile modulus E as a function of draw ratio Λ: (○) S1, (●) S2, (△) S3, (▲) S4, (□) S5, (■) S6

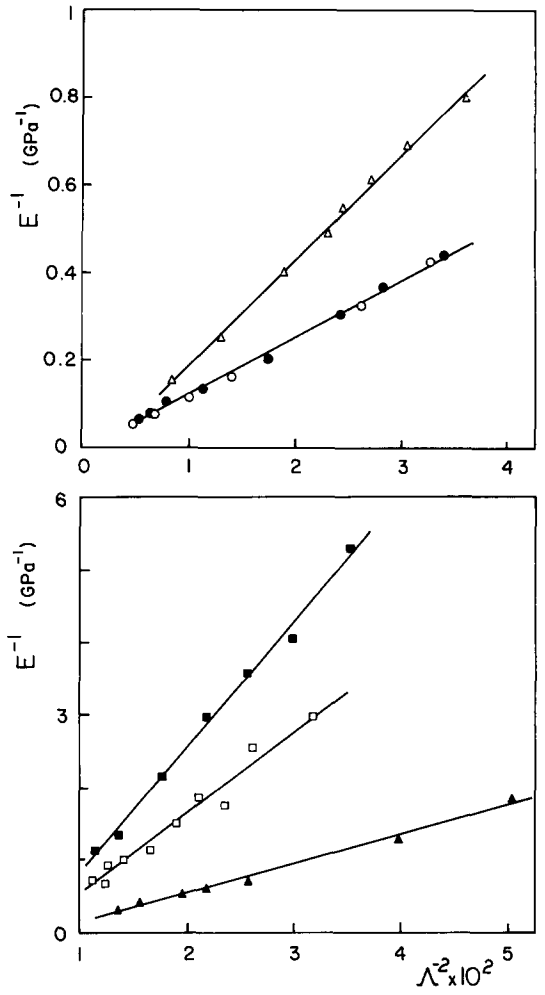

Figure 4 Plots of the compliance E^{-1} as a function of Λ^{-2} (same symbols as in *Figure 3*)

all of our samples follow very well E^{-1} *versus* Λ^{-2} linear relationships, as shown in *Figure 4*.

Determinations of the parameter f have been made in parallel with the modulus measurements. The stress–elongation curves recorded at room temperature for fibres of the six polymers drawn up to the same draw ratio $\Lambda = 10$, at 80°C, are shown in *Figure 5*. The reduced stress σ/E is reported on the ordinate axis in order to allow comparisons between the samples irrespective of the crystallinity, which affects the stiffness. Samples S3 and S4 exhibit a typical rubber stress–elongation curve with an intermediate linear domain characteristic of the asymptotic Gaussian behaviour and having a slope equal to about one-third of the initial slope. This pecularity was used in our previous study[25] for determining the fraction f in the case of a LLDPE of density $\rho = 0.930$. However, it can be seen in *Figure 5* that the ratio of the slope of the intermediate linear part to the slope at the origin of the stress–elongation curve is smaller than one-third in the case of samples S1 and S2, and greater than one-third for samples S5 and S6. The reason for this may be that the more crystalline S1 and S2 samples are prone to undergo chain slippage within the crystal phase with a concomitant creep effect. This has been clearly demonstrated by Cansfield *et al.*[29] in the case of fibres from high-density polyethylenes, for strain rates close to that used in our experiments (i.e. $d\lambda/dt = 3 \times 10^{-3} s^{-1}$). On the other hand, the low-crystallinity

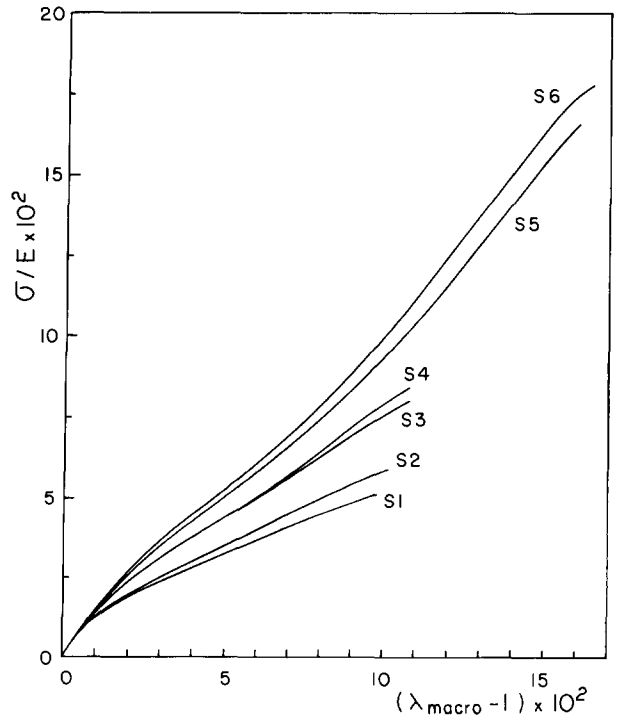

Figure 5 Reduced stress–elongation curves of fibres from the six samples drawn up to the same draw ratio $\Lambda = 10$

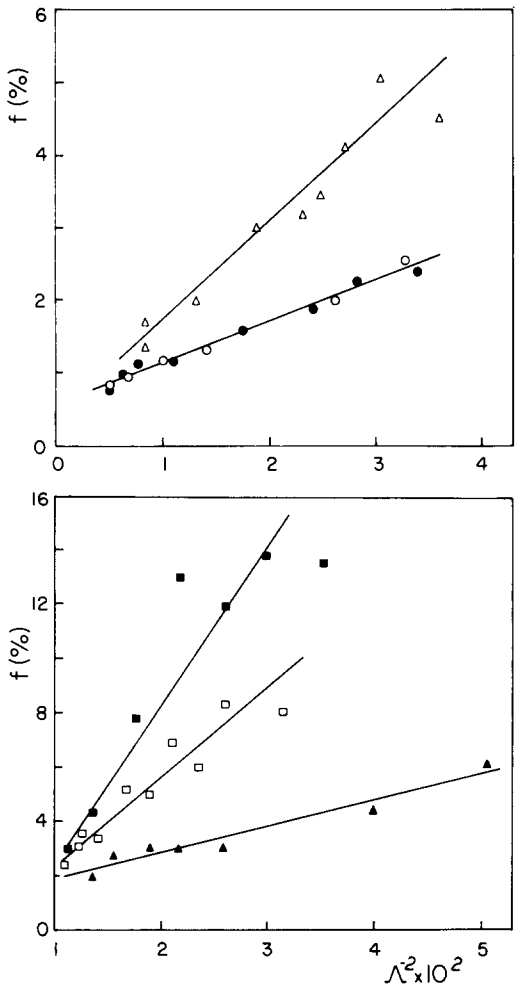

Figure 6 Plots of the fraction f as a function of Λ^{-2} (same symbols as in *Figure 3*)

samples S5 and S6 are liable to retain a higher entanglement density in the amorphous phase than the more crystalline samples, as we have already pointed out in a paper dealing with the chain topology in ethylene copolymers[30]. The strain-hardening effect due to the amorphous chain orientation is therefore expected to appear early in the stress–elongation curves of samples S5 and S6, as predicted by the theory of rubber elasticity of highly entangled networks[31]. This is why a new method of determination for f has been introduced in this paper (see the 'Theoretical considerations' section). This method has only been applied in the range of low elongation ratios of the fibres, that is for $1 < \lambda_{macro} < 1.06$, as illustrated in *Figure 2*, since it assumes Gaussian behaviour of the amorphous chains.

Figure 6 shows that the f values determined for the six samples vary according to linear relationships when plotted as a function of Λ^{-2}. An interesting conclusion can be drawn by comparing this result with the previous observation that the compliance of the fibres E^{-1} is a linear function of Λ^{-2}. Indeed, it ensues from this comparison that E^{-1} is proportional to f, for every sample studied. This general trend in the mechanical behaviour of fibres from linear polyethylenes having various crystallinities is in perfect agreement with equation (3) and gives additional credit to the model of *Figure 1* introduced in our former study dealing with a single LLDPE. It is worth noticing from *Figure 6* that $f < 0.15$ whatever the crystallinity of the starting material, in agreement with the assumption $f \ll 1$, on which equation (3) relies.

Plotting the f data as a function of the compliance E^{-1} for the six samples in *Figure 7* shows a unique and roughly linear correlation. In fact, closer examination reveals that the slope of the curve of *Figure 7* decreases from sample S1 to sample S6. Notwithstanding this, such a universal relationship is quite remarkable. It means that, from a mechanical standpoint, the parameter f takes into account both the crystallinity and the draw ratio of the fibres. Besides, the conspicuous trend of f towards zero as E^{-1} approaches zero (i.e. for very high modulus values) indicates that crystal continuity is likely to build up at very high draw ratio and high crystallinity, in agreement with Ward's model for ultra-high-modulus fibres of flexible-chain polymers (see for instance the review of ref. 32). It must be noted that our method for determining f cannot be applied in the case of crystal continuity (i.e. when $f = 0$) because of the very small residual elasticity of the fibres.

The determination of the parameter f cannot be of quantitative relevance as concerns the characterization of the fibres without measuring in parallel the fraction b of the mechanically active part in the fibres (see *Figure 1*). In our previous paper[24] we proposed a method of estimation for b, which was based on the resolution of differential scanning calorimetry curves of the fibres into lamellar and fibrillar crystal contributions to the melting. This method was successfully used in the case of LLDPE but could not be applied unambiguously in the present work either for the most crystalline samples, which display a single melting peak, or for the less crystalline ones, which exhibit very broad and complex melting curves. So, pursuing the line of our mechanical approach, it is worth pointing out that the slope of the f *versus*

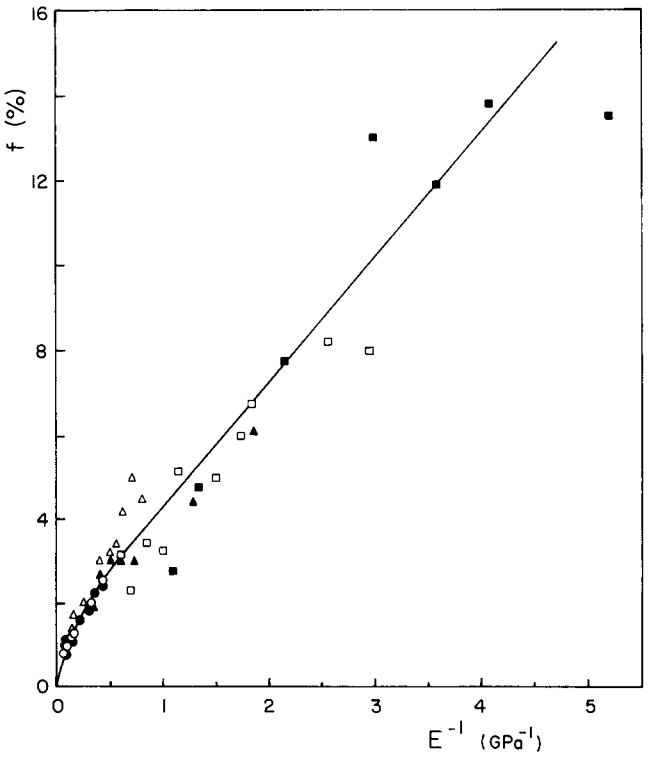

Figure 7 Universal plot of the fraction f as a function of the compliance E^{-1} (same symbols as in *Figure 3*)

Table 2 Determination of parameter b according to *Figure 7* and equation (11)

Sample	S1	S2	S3	S4	S5	S6
b	0.45	0.45	0.50	0.27	0.25	0.30

E^{-1} correlation of *Figure 7* provides a value of bE_1 for every sample, by rewriting equation (3) in the form:

$$f = bE_1E^{-1} - E_1E_c^{-1} \quad (10)$$

The negative intercept $f = -E_1E_c^{-1}$ for $E^{-1} = 0$ makes no sense from a strict physical standpoint. In fact, this merely results from the approximations introduced when deriving equation (3). If one keeps in mind that $E_1E_c^{-1}$ is very small, equation (10) appears to be fairly consistent with the data of *Figure 7*. Then the determination of b from bE_1 requires an estimation at least of E_1, which unfortunately cannot be readily obtained from experimental data. Notwithstanding this, considering that our model assumes an unstrained state of the active amorphous fraction f, it seems quite realistic to adopt the value $E_1 = 0.1\,\text{GPa}$[33], which is currently taken for the amorphous phase modulus in isotropic polyethylene. Besides, from the initial slope of the universal correlation of *Figure 7*, the above assessment of E_1 leads to $b \simeq 0.7$–0.9 for $f \to 0$, which compares favourably with the b values reported by Grubb[13] for high-modulus polyethylene fibres. The values of parameter b estimated accordingly for the six polyethylene samples are indicated in *Table 2*. Note that bE_1 has been determined from the experimental data of every sample in *Figure 7*. The decreasing trend of the parameter b from S1 to S6 which appears in *Table 2* can be understood as evidence of the reduced capability of the samples to develop a fibrillar structure under tensile drawing. This is in agreement with the lower drawability and the stronger strain-hardening effect that we have already reported for ethylene copolymers when the crystallinity decreases[34]. Both phenomena have been attributed to an increase of the entanglement density with increasing co-unit concentration in the solid samples. We suggested that this topological modification of the copolymers in parallel with their crystallinity lies in the exclusion of the co-units from the crystalline phase, which involves a greater disturbance of the chain folding process and a concomitant reduced reeling motion of the chains during the crystallization stage[30,34].

CONCLUSIONS

This study shows that the tensile modulus of fibres hot drawn from linear polyethylenes follows E^{-1} *versus* Λ^{-2} linear relationships. The measurements have been performed on six selected materials covering a wide range of crystallinities. Grubb's mechanical model for the modulus of semicrystalline polymer fibres has been satisfactorily applied in this case, at room temperature only. Every fibre can be characterized by a value of the parameter f, which represents the volume fraction of amorphous phase in the mechanically active part of the fibre. A unique f *versus* E^{-1} correlation has been obtained, which indicates that the parameter f is related to both the crystallinity and the draw ratio of the fibres. The decrease of f towards zero at low E^{-1} values is in agreement with the build-up of crystalline bridges, which has been proposed by Ward *et al.* to account for the ultra-high modulus of fibres drawing from high-density polyethylenes. Thus, the model with crystal continuity can be viewed as a limiting case of Grubb's model.

The volume fraction of the mechanically active part of the fibres falls from 0.5 to 0.25 as the crystallinity of the materials decreases. This result is in line with a previous conclusion of reduced capability of ethylene copolymers to undergo a fibrillar transformation because of topological constraints set up during the course of crystallization.

The present model deserves testing in a range of temperatures and strain rates. The problem is that our method for determining the fraction f assumes a rubbery behaviour of the mechanically active amorphous phase and neglects the deformation of the crystalline phase. On the one hand, lowering the temperatures or increasing the strain rate would cause the β relaxation in the amorphous phase to become active, making the assumption of a rubbery behaviour no longer valid, notably for the less crystalline samples. On the other hand, increasing the temperature or lowering the strain rate is expected to activate the α relaxation in the crystal, thus introducing a significant viscoelastic contribution to the deformation. This is confirmed by the slow recovery of the fibres after unloading.

ACKNOWLEDGEMENTS

The authors are indebted to the Norsolor Research Centre in Mazingarbe (France) for providing the polyethylene samples.

REFERENCES

1 Peterlin, A. in 'Man-made Fibres' (Eds. H. F. Mark, S. M. Atlas and E. Cernia), Wiley-Interscience, New York, 1967, Vol. 1, pp. 283–340
2 Peterlin, A. in 'Ultra-high Modulus Polymers' (Eds. A. Ciferri and I. M. Ward), Applied Science, London, 1979, pp. 295–301
3 Hill, M. J. and Keller, A. *J. Macromol. Sci., Phys.* (*B*) 1969, **3**, 153
4 Clark, E. S. in 'Structure and Properties of Polymer Films' (Eds. R. W. Lenz and R. S. Stein), Plenum Press, New York, 1973, pp. 267–82
5 Sprague, B. S. *J. Macromol. Sci., Phys.* (*B*) 1973, **8**, 157
6 Odell, J. A., Grubb, D. T. and Keller, A. *Polymer* 1978, **19**, 617
7 Bashir, Z., Odell, J. A. and Keller, A. *J. Mater. Sci.* 1984, **19**, 3713
8 Pennings, A. J., van der Mark, J. M. A. A. and Kiel, A. M. *Kolloid-Z. Z. Polym.* 1970, **237**, 336
9 Pennings, A. J., Lageveen, R. and De Vries, R. S. *Colloid Polym. Sci.* 1977, **255**, 532
10 Smith, J. B., Davies, G. R., Capaccio, G. and Ward, I. M. *J. Polym. Sci., Polym. Phys. Edn.* 1975, **13**, 2331
11 Barham, P. J. and Arridge, R. G. C. *J. Polym. Sci., Polym. Phys. Edn.* 1977, **15**, 1177
12 Gibson, A. G., Davies, G. R. and Ward, I. M. *Polymer* 1978, **19**, 683
13 Grubb, D. T. *J. Polym. Sci., Polym. Phys. Edn.* 1983, **21**, 165
14 Capaccio, G. and Ward, I. M. *Polymer* 1974, **15**, 233
15 Capaccio, G., Crompton, T. A. and Ward, I. M. *J. Polym. Sci., Polym. Phys. Edn.* 1980, **18**, 301
16 Zachariades, A. E., Mead, W. T. and Porter, R. S. *Chem. Rev.* 1980, **80**, 351
17 Smith, P. and Lemstra, P. J. *Polymer* 1980, **21**, 1341
18 Smook, J., Torfs, J. C., van Hutten, P. F. and Pennings, A. J. *Polym. Bull.* 1980, **2**, 293
19 Smith, P., Lemstra, P. J. and Pijpers, P. L. *J. Polym. Sci., Polym. Phys. Edn.* 1982, **20**, 2229
20 Pennings, A. J. and Smook, J. *J. Mater. Sci.* 1984, **19**, 3443
21 Hikmet, R., Lemstra, P. J. and Keller, A. *Colloid Polym. Sci.* 1987, **265**, 185
22 Hoogsteen, W., Kormelink, H., Eshuis, G., ten Brinke, G. and Pennings, A. J. *J. Mater. Sci.* 1988, **23**, 3467

23 Seguela, R. and Rietsch, F. *Polymer* 1986, **27**, 532
24 Rossignol, J. M., Seguela, R. and Rietsch, F. *Makromol. Chem., Macromol. Symp.* 1987, **9**, 27
25 Rossignol, J. M., Seguela, R. and Rietsch, F. *Polymer* 1988, **29**, 43
26 Ward, I. M. 'Mechanical Properties of Solid Polymers', 2nd Edn., Wiley-Interscience, New York, 1985, Ch. 4
27 Jareki, L. and Meier, D. J. *J. Polym. Sci., Polym. Phys. Edn.* 1979, **17**, 1611
28 Leung, W. P., Choy, C. L., Xu, C., Qi, Z. and Wu, R. *J. Appl. Polym. Sci.* 1988, **36**, 130
29 Cansfield, D. L. M., Ward, I. M., Woods, D. W., Buckley, A., Pierce, J. M. and Wesley, J. L. *Polym. Commun.* 1983, **24**, 130
30 Seguela, R. and Rietsch, F. *J. Mater. Sci.* 1988, **23**, 415
31 Treloar, L. R. G. 'The Physics of Rubber Elasticity', 2nd Edn., Clarendon Press, Oxford, 1958
32 Ward, I. M. *Adv. Polym. Sci.* 1985, **70**, 1
33 Sakurada, I., Kaji, K. and Wadano, S. *Colloid Polym. Sci.* 1981, **259**, 1208
34 Seguela, R. and Rietsch, F. *Polymer* 1986, **27**, 703